Journal of Medicinal Chemistry

Article

pubs.acs.org/jmc

Copper(II) Complexes of Salicylic Acid Combining Superoxide Dismutase Mimetic Properties with DNA Binding and Cleaving Capabilities Display Promising Chemotherapeutic Potential with Fast Acting in Vitro Cytotoxicity against Cisplatin Sensitive and Resistant Cancer Cell Lines

Mark O'Connor,[†,⊥] Andrew Kellett,[†,#] Malachy McCann,[‡] Georgina Rosair,[§] Mary McNamara,[†] Orla Howe,[†] Bernadette S. Creaven,[∥] Siobhán McClean,[∥] Agnieszka Foltyn-Arfa Kia,[∥] Denis O'Shea,[†] and Michael Devereux*[,†]

[†]The Inorganic Pharmaceutical and Biomimetic Research Centre, Focas Research Institute, Dublin Institute of Technology, Camden Row, Dublin 8, Ireland

[‡]Chemistry Department, National University of Ireland, Maynooth, County Kildare, Ireland

[§]School of Engineering and Physical Sciences, Heriot Watt University, Edinburgh EH14 4AS, U.K.

[∥]Centre of Applied Science for Health, Institute of Technology Tallaght Dublin, Tallaght, Dublin 24, Ireland

Supporting Information

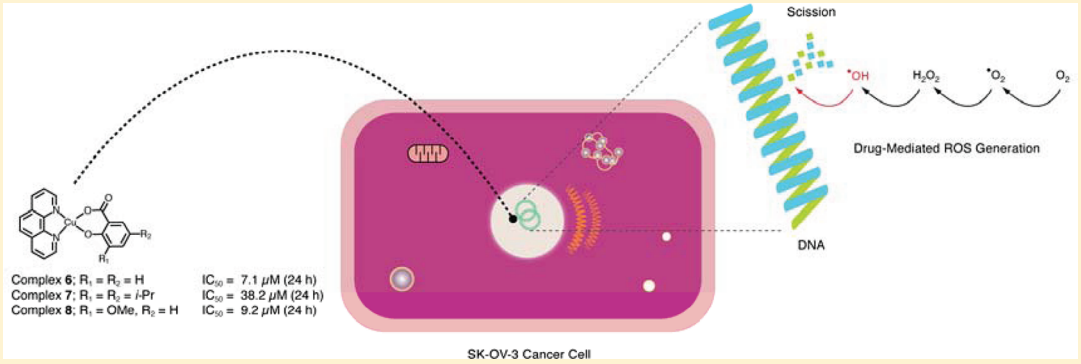

ABSTRACT: The complexes $[Cu(salH)_2(H_2O)]$ (**1**), $[Cu(dipsH)_2(H_2O)]$ (**2**), $\{Cu(3\text{-}MeOsal)(H_2O)_{0.75}\}_n$ (**3**), $[Cu(dipsH)_2(BZDH)_2]$ (**4**), $[Cu(dipsH)_2(2\text{-}MeOHBZDH)_2]\cdot EtOH$ (**5**), [Cu(sal)(phen)] (**6**), $[Cu(dips)(phen)]\cdot H_2O$ (**7**), and $[Cu(3\text{-}MeOsal)(phen)]\cdot H_2O$ (**8**) ($salH_2$ = salicylic acid; $dipsH_2$ = 3,5-diisopropylsalicylic acid; $3\text{-}MeOsalH_2$ = 3-methoxysalicylic acid; BZDH = benzimidazole; 2-MeOHBZDH = 2 methanolbenzimidazole and phen =1,10-phenanthroline) were prepared and characterized. Structures of **4**, **5**, and **8** were determined by X-ray crystallography. Compounds **1**−**8** are potent superoxide dismutase mimetics, and they are inactive as inhibitors of COX-2 activity. Compounds **1**, **4**, and **5** exhibit moderate inhibition of COX-1. Complexes **6**−**8** display rapid micromolar cytotoxicity against cisplatin sensitive (breast (MCF-7), prostate (DU145), and colon (HT29)) and cisplatin resistant (ovarian (SK-OV-3)) cell lines compared to **1**−**5**, and they exhibit potent in vitro DNA binding and cleavage capabilities.

1. INTRODUCTION

There is growing evidence demonstrating the role of inflammation in cancer initiation, progression, and metastasis.[1] Sustained cell proliferation in an environment rich in inflammatory cells, growth factors, activated stroma, and DNA-damage-promoting agents is now known to promote neoplastic risk. In wounds resulting from tissue damage, cell proliferation increases while the tissue regenerates; proliferation and inflammation subside after the repair is completed. However, when DNA damage and/or mutagenic assault persists, cells will continue to proliferate in microenvironments rich in inflammatory cells and survival factors that support their growth and tumors can result where such wounds fail to heal.[2] Inflammatory conditions can precede a malignant change during tumor formation or in some types of cancers; an oncogenic change encourages an inflammatory response which promotes the development of tumors.[3] Prolonged inflammation in the tumor microenvironment has many tumor-promoting effects such as: (i) aiding in the proliferation and

Received: August 3, 2011
Published: February 7, 2012

dx.doi.org/10.1021/jm201041d | J. Med. Chem. 2012, 55, 1957−1968

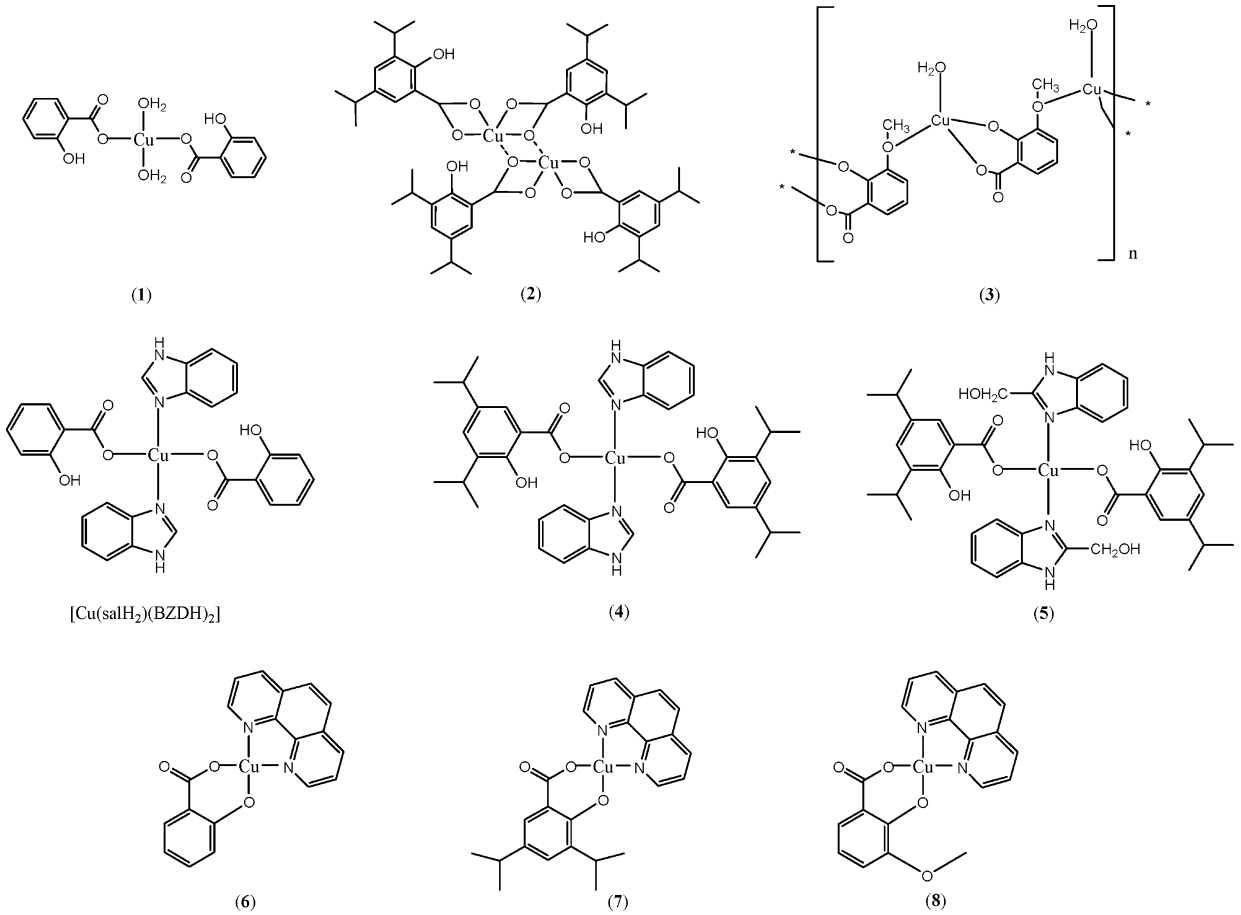

Figure 1. Proposed structures of the complexes **1**–**8** and $[Cu(salH_2)_2(BZDH)_2]$.

survival of malignant cells, (ii) promoting angiogenesis and metastasis, (iii) subverting adaptive immune responses, and (iv) altering responses to hormones and chemotherapeutic agents. Drugs that are able to inhibit both inflammation and cancer are of great interest for clinical use.

A considerable body of evidence suggests that formation of potent reactive oxygen species (ROS) and resultant oxidative stress plays a major role in inflammation and that it contributes to carcinogenesis. During acute and chronic inflammation, the superoxide radical ($O_2^{\bullet-}$) is produced in excess and the endogenous superoxide dismutase (SOD) enzyme defense system is overwhelmed and unable to effectively remove it, resulting in a pro-inflammatory response and in superoxide-mediated cellular injury.[4,5] Furthermore, many tumor cells have increased rates of metabolism compared with normal cells, which would typically lead to increased numbers of ROS such as the superoxide radical.[6] This biochemical imbalance may be further exacerbated in tumors, as the activities of mitochondrial manganese SOD (MnSOD) and cytoplasmic CuZnSOD have been shown to be depleted in cancer cells, suggesting the resultant excess $O_2^{\bullet-}$ can further metabolize to peroxynitrite ($OONO^-$), which plays a key role in inflammation and pain.[7,8] The excess superoxide may also metabolize to form the perhydroxyl radical ($HO_2^{\bullet}$) which, along with the peroxynitrite, plays a role in the tumor formation.[4] When tested in humans in various clinical trials, bovine CuZnSOD showed promising anti-inflammatory effects under acute and chronic conditions including rheumatoid arthritis and osteoarthritis as well as the deleterious side effects associated with chemotherapy and radiation therapy.[9] Furthermore, it has been demonstrated that returning MnSOD and CuZnSOD enzyme activity to levels close to those found in nonmalignant cells has resulted in conversion of the excess $O_2^{\bullet-}$ to H_2O_2 (which is converted in turn to the cytotoxic hydroxyl radical ($OH^{\bullet}$)), which leads to decreased tumor cell growth in a number of model systems.[10−12] The cytotoxicity of the hydroxyl radical ($OH^{\bullet}$) is related to its ability to induce protein oxidation, lipid peroxidation, and oxidative DNA damage. The native SOD enzyme thus has therapeutic potential to modulate the course of inflammation and kill cancer cells. The use of SOD enzymes as pharmaceutical agents is limited by cost and because of instability and low membrane permeability resulting from their high molecular weight. Low molecular weight copper SOD mimetic complexes can dismutate excess intracellular $O_2^{\bullet-}$ to H_2O_2 and O_2, suggesting that they replicate the anti-inflammatory activity of endogenous SOD enzymes and they may increase the concentration of H_2O_2 in cancer cells, thus inducing cell death by apoptosis. A number of copper SOD mimetics have been shown to possess anti-inflammatory[13] and antitumor activity.[14]

Salicylic acid ($salH_2$) and its derivatives are known nonsteroidal anti-inflammatory drugs (NSAIDs). Their pharmacological activity has been attributed to their ability to block the action of the enzyme cyclooxygenase (COX), which is present in two forms, COX-1 and COX-2.[15] Recent research has shown that the COX-2 isoenzyme is overexpressed in colon cancer cells and has been linked to an increase in angiogenisis, increased tumor invasiveness, and also a decrease in apoptosis

dx.doi.org/10.1021/jm201041d | J. Med. Chem. 2012, 55, 1957−1968

of the cancer cell.[16] Inhibition of the COX-2 enzyme has been found to delay tumor growth as well as improving response to conventional cancer therapies.[17] A study of cancer risk among long-term users of NSAIDs such as salicylic acid and aspirin (acetyl salicylic acid) is perhaps the best evidence for the significance of inflammation during neoplastic progression. The data indicates that use of these drugs reduces colon cancer risk by 40−50% and may be preventative for lung, esophagus, and stomach cancer.[18,19] Copper complexes of salicylic acid are potent SOD mimetics,[13] and they are known to be more potent anti-inflammatory agents than the uncoordinated NSAID itself and they have been shown to have low toxicity and less side effects as evidenced by their successful long-term applications in veterinary medicine.[20,21] In 1990, Sorenson and Oberley demonstrated the anticancer potential of copper salicylate SOD mimetic complexes in animal models where treatments resulted in decreased tumor growth, increased survival of the host organism, decreased tumor metastasis, and induced morphological differentiation of cancerous cells.[22]

In our laboratories, we have recently demonstrated that the copper(II) complexes $[Cu(salH)_2(H_2O)_2]$, [Cu(sal)(phen)], and $[Cu(salH)_2(BZDH)_2]$ {phen =1,10-phenanthroline and BZDH = benzimidazole} (Figure 1) are comparable potent SOD mimetics which induce a range of in vitro cytotoxicities when hepatic (*Hep-G*$_2$), renal (*A-498*), and lung (*A*-549) cancer cell lines are exposed to them for 96 h.[23] Whereas $[Cu(salH)_2(H_2O)_2]$ and $[Cu(salH)_2(BZDH)_2]$ were found to be significantly less active than the clinical drug cisplatin against the three cell lines tested, [Cu(sal)(phen)] in turn was 6, 9, and 8 times more active than the clinical drug against the cell lines, respectively. The lack of correlation between the SOD activities and cytotoxicity properties of $[Cu(salH)_2(H_2O)_2]$, [Cu(sal)(phen)], and $[Cu(salH)_2(BZDH)_2]$ indicates that mechanisms other than SOD mimicking must also be contributing to the anticancer properties of these complexes. Furthermore, the order of cytotoxic activity of these water insoluble complexes ([Cu(sal)(phen)] ≫ $[Cu(salH)_2(BZDH)_2]$ > $[Cu(salH)_2(H_2O)_2]$) suggests that the chelating nature of the sal^{2-} and phen ligands may enhance the cytotoxicity of [Cu(sal)(phen)]. These preliminary results have prompted us to examine this class of complex further in an effort to throw some light on the relationship between their structure and their chemotherapeutic potential. Herein, we detail the preparation, SOD and catalase mimetic activities, the isolated COX-1 and COX-2 inhibitory capabilities, the DNA binding and nuclease activities, and the anticancer chemotherapeutic potential of $[Cu(salH)_2(H_2O)_2]$ (**1**), $[Cu(dipsH)_2(H_2O)]$ (**2**), $\{Cu(3\text{-}MeOsal)(H_2O)_{0.75}\}_n$ (**3**), $[Cu(dipsH)_2(BZDH)_2]$ (**4**), $[Cu(dipsH)_2(2\text{-}MeOHBZDH)_2]\cdot EtOH$ (**5**), [Cu(sal)(phen)] (**6**), $[Cu(dips)(phen)]\cdot H_2O$ (**7**), and $[Cu(3\text{-}MeOsal)(phen)]\cdot H_2O$ (**8**) (3-MeOsalH_2 = 3-methoxysalicylic acid, 2-MeOHBZDH = 2-methanolbenzimidazole). The X-ray crystal structures of $[Cu(dipsH)_2(BZDH)_2]$ (**4**), $[Cu(dipsH)_2(2\text{-}MeOHBZDH)_2]\cdot EtOH$ (**5**), and $[Cu(3\text{-}MeOsal)(phen)]\cdot H_2O$ (**8**) are also reported.

2. RESULTS AND DISCUSSION

2.1. Synthesis and Characterization of the Compounds. Complexes **1** and **6** were generated using methods described previously.[24] The copper(II) salicylate complexes $[Cu(dipsH)_2(H_2O)]$ (**2**) and $\{Cu(3\text{-}MeOsal)(H_2O)_{0.75}\}_n$ (**3**) were prepared by reacting copper(II) hydroxide with the respective salicylic acid in ethanol. $[Cu(dipsH)_2(BZDH)_2]$ (**4**), $[Cu(dipsH)_2(2\text{-}MeOHBZDH)_2]\cdot EtOH$ (**5**), $[Cu(dips)(phen)]\cdot H_2O$ (**7**), and $[Cu(3\text{-}MeOsal)(phen)]\cdot H_2O$ (**8**) were generated by reacting the respective copper(II) salicylates **1**, **2**, and **3** with either the relevant benzimidazole or 1,10-phenanthroline in ethanol. Complexes **1**−**8** were characterized by infrared spectroscopy, elemental analysis, magnetic susceptibility, molar conductivity measurements, and their solid/solution-state UV−vis spectra. The physicochemical properties for **1** are the same as those for a compound that was previously reported for which the crystal structure revealed a square planar geometry with the salicylate ligands trans to one another and bound through the carboxylate groups in a monodentate fashion.[25] The proposed structures for the complexes are shown in Figure 1.

Complexes **1**−**8** were found to be insoluble in all common solvents but, with the exception of **3**, were soluble in DMSO. The benzimidazole derivatives **4** and **5** exhibit significant shifts of the d−d transition bands (563 nm →733 nm (**4**), 575 nm → 740 nm (**5**), respectively) in their DMSO solution spectra as compared to the solid state, and therefore some structural change in the complexes is believed to be taking place in solution. The remaining complexes exhibit only small shifts of their d−d transition bands in their DMSO solution spectra as compared to the solid state, and therefore no real change in the complex is taking place in solution. The molar conductivity values of the soluble complexes in DMSO fall below the range expected for 1:1 electrolytes (50−70 S cm^2 mol^{-1}), suggesting that no significant dissociation of the complexes is taking place.

In the IR spectra of all eight complexes, new bands at 1633−1552 and 1472−1384 cm^{-1} are assigned to asymmetric and symmetric stretching vibrations of the coordinated carboxylate groups indicative of the presence of the salicylate ligands. In the IR spectrum of complex **2**, the carboxylate bands are split (ν_{asym}(OCO), 1628 cm^{-1} and 1592 cm^{-1}; ν_{sym}(OCO), 1468 cm^{-1} and 1390 cm^{-1}), indicative of the presence of two different modes of coordination for the salicylate carboxylate groups. A manganese(II) salicylate complex reported by this group[26] formulated as $[Mn_2(salH)_4(H_2O)_2]$ (salH$_2$ = salicylic acid) exhibits similar physicochemical properties to that of **2**. It too has its asymmetric and symmetric OCO bands split in the IR spectrum. Furthermore, the IR spectra of complex **2** and $[Mn_2(salH)_4(H_2O)_2]$ both exhibit bands in the region 840−820 cm^{-1}, which are not found in the spectrum of the respective carboxylic acids and which are characteristic of coordinated water molecules.[27] There is significant metal−metal interaction in **2**, having a subnormal room temperature magnetic moment of 1.38 μ_B.[28] On this basis, it is possible that **2** has a binuclear structure similar to that of $[Mn_2(salH)_4(H_2O)_2]$.

Complex **3** formulates as having just one 3-methoxysalicylate ligand per copper. The presence of the methoxy group is confirmed in the infrared spectrum by the C−O−C band at 1061 cm^{-1}. This band has shifted from 1055 cm^{-1} in the spectrum of the metal free 3-methoxysalicylic acid and has lost significant intensity, and therefore it is proposed that the ethereal oxygen is involved in coordination to the copper center. The complex also formulates as having water in its structure, and a typical M−OH$_2$ band at 835 cm^{-1} in the IR spectrum is indicative of a water molecule coordinated to the metal center.[27] Although **3** has a normal room temperature magnetic moment (1.65 μ_B), its relative insolubility suggests that it may be polymeric in nature.

dx.doi.org/10.1021/jm201041d | J. Med. Chem. 2012, 55, 1957−1968

Bands that are characteristic of salicylate anions are found in the IR spectra of complexes **4** (ν_{asym}(OCO), 1618 cm^{-1}; ν_{sym}(OCO), 1362 cm^{-1}) and **5** (ν_{asym}(OCO), 1552 cm^{-1}; ν_{sym}(OCO), 1388 cm^{-1}), and they also contain the typical bands indicative of bound benzimidazoles. The Δ_{OCO} value of 256 cm^{-1} for **4** is in agreement with the observed crystal structure (Figure 2), which clearly shows a monodentate

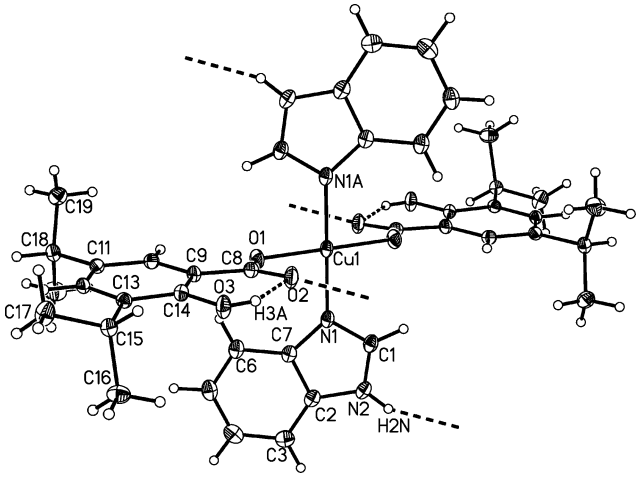

Figure 2. The X-ray structure and atom numbering scheme for [Cu(dipsH)$_2$(BZDH)$_2$] (**4**).

coordination mode for the salicylate carboxylate groups.[27] The Δ_{OCO} value of 164 cm^{-1} for **5** is lower than expected for monodentate coordination mode, but such relative reduction in the Δ_{OCO} values are typical where carboxylate groups are involved in extensive intra- and/or intermolecular hydrogen bonding as is observed in the molecular structure for **5** (Figure 3). Complexes **4** and **5** both have normal room temperature

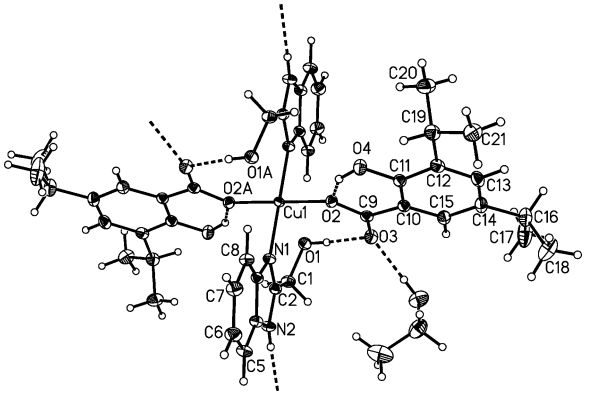

Figure 3. The X-ray structure and atom numbering scheme for [Cu(dipsH)$_2$(2-MeOHBZDH)$_2$]·EtOH (**5**).

magnetic moments (1.69 μ_B and 1.79 μ_B, respectively) as would be expected for such mononuclear copper(II) complexes.[28]

The IR spectra of complexes **6**, **7**, and **8** contain absorption bands which are characteristic of the presence of chelating phen ligand (846 cm^{-1} and 721 cm^{-1} (**6**), 845 cm^{-1} and 724 cm^{-1}(**7**), and 847 cm^{-1} and 722 cm^{-1} (**8**)).[29] As well as the bands that have been assigned to the chelating phen ligand, the spectra of the three complexes also contain bands that are characteristic of salicylate anions with ν_{asym}(OCO) (1599 cm^{-1} (**6**), 1612 cm^{-1} (**7**) and 1572 cm^{-1} (**8**)) and ν_{sym}(OCO) (1384 cm^{-1} (**6**), 1454 cm^{-1} (**7**) and 1445 cm^{-1} (**8**)) bands. The normal room temperature magnetic moments of 2.11 μ_B (**6**), 2.05 μ_B (**7**), and 1.85 μ_B (**8**) are consistent with a structure lacking Cu−Cu interactions.[28] In view of the similarity of the IR and electronic spectra, it is proposed that **6** and **7** adopt the same square planar structure as observed for [Cu(3-MeOsal)(phen)]·H_2O (**8**) (Figure 4).

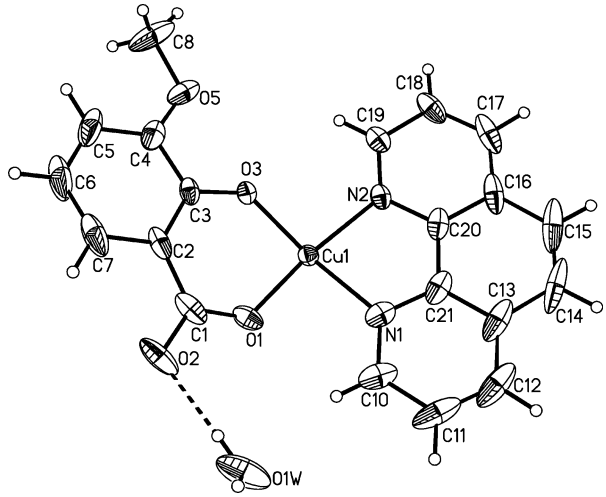

Figure 4. The X-ray structure and atom numbering scheme for [Cu(3-MeOsal)(phen)]·H_2O (**8**).

2.2. X-Ray Studies. The three complexes **4**, [Cu(dipsH)$_2$(2-MeOHBZDH)$_2$]·EtOH (**5**), and **8** were obtained as crystals suitable for X-ray analysis and their structures were determined. [Cu(dipsH)$_2$(BZDH)$_2$] (**4**) and [Cu(dipsH)$_2$(2-MeOHBZDH)$_2$]·EtOH (**5**) both have square planar copper centers which lie on centers of inversion, and their structures are quite similar (shown in Figures 2 and 3, respectively). They both contain N_2O_2 ligation with two trans benzimidazole and two monodentate salicylate ligands. Benzimidazole ligands from neighboring molecules lie above and below the vacant axial sites at the Cu center in **4**, whereas in **5** the intramolecular benzimidzole methanol substituent O atoms are 2.503(2) Å either side of the copper center.

The protonated benzimidazole nitrogen in both complexes is capable of hydrogen bonding and consequently intermolecular NH···O hydrogen bonds with the neighboring carboxylate O atoms are observed in both cases. In both **4** and **5**, there are intramolecular hydrogen bonds between the phenoxy O−H groups and the uncoordinated carboxylate O atoms of each of the 3,5-diisopropylsalicylate ligands. However, in **5**, there are further interligand intramolecular hydrogen bonds, where the MeOH substituents on the benzimidazole 2 position make an OH···O hydrogen bond with the uncoordinated carboxylate oxygen atoms. This oxygen atom, O3, and its symmetry equivalent, in turn make intermolecular O···HO hydrogen bonds with the solvent.

[Cu(3-MeOsal)(phen)]·H_2O (**8**) (Figure 4) is closely related to [Cu(sal)(bipy)]·EtOH·H_2O which was previously published.[23] The bond lengths are very similar, e.g., Cu−O(carboxylate) 1.8976(15) cf. 1.893(2)Å in **8**. The copper(II) ion is coordinated to the two nitrogen donors of the phen ligand and chelated by the salicylate dianion via one carboxylate oxygen atom and the phenolate oxygen atom, giving the copper atom an approximate square planar geometry. While **4** and **5**

dx.doi.org/10.1021/jm201041d | J. Med. Chem. 2012, 55, 1957−1968

Table 1. IC_{50} Values (μM) Obtained for Complexes 1−8 and the Clinically Used Antitumor Agent Cisplatin against Breast (MCF-7), Prostate (DU145), Ovarian (SK-OV-3), and Colon (HT29) Cancer Cell Lines over 24 and 96 h Time Periods

	antitumor activity IC_{50} (μM) ± SEM							
	MCF-7		DU145		SK-OV-3		HT29	
	24 h	96 h	24 h	96 h	24 h	96 h	24 h	96 h
$salH_2$	>100	>100	>100	>100	>100	>100	>100	>100
$dipsH_2$	>100	>100	>100	>100	>100	>100	>100	>100
$msalH_2$	>100	>100	>100	>100	>100	>100	>100	>100
BZDH	>100	>100	>100	>100	>100	>100	>100	>100
2-MeOHBZDH	>100	>100	>100	>100	>100	>100	>100	>100
1	>100	>100	>100	>100	>100	>100	>100	>100
2	>100	78.3 ± 8.6	>100	64.7 ± 5.7	>100	>100	>100	>100
3	>100	>100	>100	>100	>100	>100	>100	>100
4	>100	71.2 ± 8.0	>100	53.7 ± 5.5	>100	>100	>100	71.7 ± 8.6
5	>100	23.9 ± 4.5	>100	60.5 ± 2.8	>100	>100	>100	74.7 ± 8.1
6	49.3 ± 2.1	5.3 ± 1.6	7.8 ± 1.2	6.2 ± 0.3	7.1 ± 0.5	4.8 ± 0.5	11.2 ± 2.1	3.07 ± 0.5
7	32.6 ± 4.3	6.6 ± 1.1	28.3 ± 2.1	6.0 ± 0.2	37.4 ± 2.0	3.8 ± 0.4	47.7 ± 5.2	6.1 ± 1.3
8	47.5 ± 3.0	5.8 ± 0.9	8.4 ± 0.9	4.5 ± 0.4	9.2 ± 0.6	2.9 ± 0.6	12.9 ± 3.4	2.8 ± 1.1
cisplatin	90.8 ± 3.5	72.5 ± 3.3	>500	8.6 ± 0.7	>500	37.1 ± 10	348.6 ± 81	72.1 ± 1.5
phen	325.3 ± 65	6.2 ± 0.8	281.0 ± 6.9	6.0 ± 0.3	292.0 ± 26	16.1 ± 5.7	358.0 ± 10.1	5.6 ± 0.5
Cu^{2+} (as a salt)	>100	>100	>100	>100	>100	>100	>100	>100

are both monomers, there is a long Cu···O (2.462(2) Å) contact with a neighboring molecule which gives rise to a centrosymmetric dimer. The lattice water molecule makes hydrogen bonds with the uncoordinated carboxylate oxygen (O2) of one molecule of **8** and the coordinated carboxylate oxygen (O1) of another molecule. These interactions propagate a chain along the [10−1] direction. The phen rings interdigitate either side of these chains, with some evidence of weak π-stacking interactions present (intercentroid distance 3.651(2) Å between N1/C10/C11/C12/C13/C21 and N2/C19/C18/C17/C16/C20).

2.3. In Vitro Anticancer Activity. The cytotoxic properties of the complexes **1**−**8** and their free ligands along with the clinically used drug cisplatin were investigated using a standard MTT assay against four human derived cell lines (breast (MCF-7), prostate (DU145), ovarian (SK-OV-3), and colon (HT29)). It should be noted that ovarian adenocarcinoma (SK-OV-3) cells are resistant to tumor necrosis factor and to several cytotoxic drugs including cisplatin. In addition, colorectal adenocarcinoma HT29 malignancies have proven difficult to treat with cisplatin. The free ligands, the simple salicylate complexes **1**−**3**, and the benzimidazole derivatives **4** and **5** all exhibited IC_{50} values in excess of 100 μM against all four tumor cell lines over the 24 h exposure (Table 1). Furthermore, free Cu^{2+} ions (as a copper(II) salt) were found to be noncytotoxic at concentrations up to 100 μM. Representative cytotoxicity plots following 96 h treatments for the four individual cell lines for the three phen complexes **6**−**8** are included in Supporting Information Figure S1. After a 96 h exposure, complexes **2**, **4**, and **5** exhibit some moderate activity against the breast, prostate, and colon (for **4** and **5**) cell lines and the "metal free" phen ligand exhibits potent activity against all four cell lines. In contrast, complexes **6**−**8** containing the chelating phen ligand exhibited rapid low-micromolar cytotoxicity over 24 h (Table 1), with their activity improving significantly when all four cancer cells are exposed to the complexes for 96 h. Complexes **6** and **8** have very similar activity profiles. Although complex **7** is marginally more active against the breast cancer cell line than **6** and **8**, over a 24 h exposure, it is approximately four times less active against the prostate, ovarian, and colon cancer cells over this time frame. The activities of complexes **6**−**8** are remarkable given that they are observed after just 24 h, as it is generally accepted that cells should be exposed to potential cytotoxic agents for a reasonable period of time (typically 72−96 h) to allow the compounds to reach DNA or another biological target. Indeed, the relatively low activity of cisplatin over the 24 h exposure may result from the need for it to hydrolyze, in the cell cytoplasm, to the cytotoxic $[Pt(NH_3)_2(OH)_2]$, which is known to take between 48 and 96 h post intravenous injection.[30] Finally, these complexes also exhibit similar significant rapid activity toward the cisplatin resistant ovarian cell line, indicating that their activity is not influenced by the platinum drug resistant mechanisms in the SK-OV-3 cell line.

The tumor suppressor gene *p53* is known to become mutated in many human cancers, including the cisplatin resistant colorectal (HT29) and prostate (DU145) cell lines. It has been demonstrated that "metal free" phen enhances *p53* activity in vitro and can trigger apoptosis in *p53* negative cell lines.[31,32] Previously, we have observed that after exposure for 96 h phen exhibits substantially greater in vitro cytotoxicity than cisplatin against selected liver, lung, and kidney cancer cell lines.[23,33,34] Again, the low activity observed for "metal free" phen after the 24 h exposure (Table 1) may indicate that the complexes **6**−**8** do not derive their cytotoxicity simply from the presence of the phen ligand. Phen and its substituted derivatives have high affinities for copper ions,[35,36] and copper complexes of phen have been shown to exhibit excellent antitumor,[22] antifungal,[24] and antibacterial[31] activities.

2.4. SOD and Catalase Activity. The SOD mimetic activities of the complexes were determined using an indirect method in which the xanthine/xanthine oxidase system served as the source of superoxide radicals. The activities of the complexes were compared to that of $[Cu_2(indo)_4(H_2O)_2]$ (indoH = the NSAID indomethacin [1-(4-chlorobenzoyl)-5-methoxy-2-methyl-1*H*-indole-3-acetic acid]), which is considered to be an excellent SOD mimetic[37] and which is used therapeutically as an oral anti-inflammatory drug in veterinary medicine.[13,38] The results are given in Table 2 as concentrations equivalent to effect one unit of SOD activity (IC_{50} values). All of the complexes showed excellent activity with one

dx.doi.org/10.1021/jm201041d | J. Med. Chem. 2012, 55, 1957−1968

Table 2. Superoxide Dismutase (SOD) Activities of Complexes 1−8

complex	concentration (μM) equivalent to effect 1U SOD (IC_{50})
$[Cu(salH)_2(H_2O)_2]$ (**1**)	1.23
$[Cu(dipsH)_2(H_2O)_2]$ (**2**)	1.16
$\{Cu(3\text{-}MeOsal)(H_2O)_{0.75}\}_n$ (**3**)	1.42
$[Cu(dipsH)_2(BZDH)_2]$ (**4**)	0.94
$[Cu(dipsH)_2(2\text{-}MeOHBZDH)_2]\cdot EtOH$ (**5**)	1.29
[Cu(sal)(phen)] (**6**)	1.01
$[Cu(dips)(phen)]\cdot H_2O$ (**7**)	1.23
$[Cu(3\text{-}MeOsal)(phen)]\cdot H_2O$ (**8**)	1.72
$[Cu_2(indo)_4(H_2O)_2]$[37]	1.31
$CuSO_4$	30.00

unit of SOD activity arising from the range 0.94−1.72 μM comparable to the $[Cu_2(indo)_4(H_2O)_2]$. It is noteworthy that the derivatization of the salicylate complexes **1**, **2**, and **3** with either monodentate benzimidazole or chelating phen ligands does not significantly enhance their SOD mimetic activities. The lack of correlation between the SOD and cytotoxicity IC_{50} values for complexes **6**−**8** supports the notion that mechanisms other than SOD mimicking may also be responsible for the anticancer properties of these three complexes.

A small number of copper carboxylate complexes have recently been reported in the literature that show significant catalase mimetic functionality.[39,40] Such activity is not desirable where copper complexes are to be used as SOD mimetics as they may catalytically disproportionate the H_2O_2 generated during the SOD activity to water and molecular oxygen rather than react with it to form the desirable cytotoxic hydroxyl radical (Fenton chemistry). Complexes **1**−**8** were found to be inactive toward the disproportionation of hydrogen peroxide when tested in the absence of added imidazole, with poor activity observed in the presence of the base (Supporting Information Table S1).

2.5. COX Inhibition. The anticancer activity of acetylsalicylic acid (aspirin) has been attributed, in part, to its effects on cyclooxygenases, and it is known to exhibit weaker inhibition of COX-2 than COX-1.[41] Aspirin has a relatively short half-life in human plasma, as it is rapidly converted to the salicylate anion by deacetylation, and it is likely that its anti-inflammatory and anticancer properties are due to the action of the salicylate which is known to have very weak anti-COX-1 or anti-COX-2 activities. The cyclooxygenase inhibitory profile of complexes **1**−**8** was examined using the Cayman COX assay kit (results shown in Table 3). The Cayman COX assay directly measures the prostanoid product PGF_2 by $SnCl_2$ reduction of COX derived prostaglandin (PGH_2) produced in the COX reaction. Salicylic acid exhibits only marginal activity toward COX-1 (26.5% inhibition) and is inactive as a COX-2 inhibitor in this assay. Similarly, complexes **1**−**8** are inactive toward COX-2 and only complexes **1**, **4**, and **5** exhibit any COX-1 inhibition (11.6%, 37.5%, and 27.78%, respectively). Interestingly, the highly cytotoxic bis-chelate ($salicylate^{2-}$/phen) complexes **6**, **7**, and **8** appear to be completely void of cyclooxygenase inhibitory activity and therefore it is assumed that their effects on cyclooxygenases do not play a part in their mode of action.

2.6. DNA Binding Properties. The effectiveness of many anticancer agents depends on the mode and affinity of their binding with DNA.[42] In an effort to throw some light on the cytotoxicity profile of complexes **1**−**8**, their ability to interact

Table 3. COX Inhibitory Effects at a Concentration of 10 μM

compd	COX-1 inhibition (%)	COX-2 inhibition (%)
$[Cu(salH)_2(H_2O)_2]$ (**1**)	11.6	0
$[Cu(dipsH)_2(H_2O)_2]$ (**2**)	0	0
$\{Cu(3\text{-}MeOsal)(H_2O)_{0.75}\}_n$ (**3**)	0	0
$[Cu(dipsH)_2(BZDH)_2]$ (**4**)	37.50	0
$[Cu(dipsH)_2(2\text{-}MeOHBZDH)_2]\cdot EtOH$ (**5**)	28.78	0
[Cu(sal)(phen)] (**6**)	0	0
$[Cu(dips)(phen)]\cdot H_2O$ (**7**)	0	0
$[Cu(3\text{-}MeOsal)(phen)]\cdot H_2O$ (**8**)	0	0
salicylic acid	26.50	0

DNA was assessed using a competitive ethidium bromide (EtBr) displacement experiment which allowed comparison with the known DNA intercalator actinomycin D and the DNA minor groove binder pentamadine, using calf thymus DNA (CT-DNA). Et^+ bound DNA is highly flourgenic, and in the presence of excess Et^+, binding regions within the DNA polymer become saturated. Thus, during competitive displacement, an exogenous reagent must "compete" at the binding site with Et^+, resulting in a sequential reduction in fluorescence. Actinomycin D and pentamidine are highly efficient in the displacement of Et^+ bound DNA and, as expected, their apparent binding constants (K_{app}) are high (Table 4).

Table 4. Apparent DNA Binding Constants (K_{app}) of 6−8 along with Actinomycin D and Pentamidine[a]

drug/complex	C_{50}[b] (μM)	K_{app}[c]
actinomycin D	10.89	9.69×10^5
pentamidine	15.44	6.07×10^5
[Cu(sal)(phen)] (**6**)	53.48	2.24×10^5
$[Cu(dips)(phen)]\cdot H_2O$ (**7**)	120.78	9.91×10^4
$[Cu(3\text{-}MeOsal)(phen)]\cdot H_2O$ (**8**)	50.48	2.37×10^5

[a]Assay conditions: final volume 2 mL, 1.2 μM EtBr, 1 μM CT-DNAp, 10 mM TES, 0.1 mM Na_2EDTA, pH 7.0. [b]C_{50} = concentration required to reduce fluorescence by 50% [c]$K_{app} = K_e \times 1.26/C_{50}$ where $K_e = 9.5 \times 106$ $M(bp)^{-1}$

Complexes **1**−**5** showed no ability to interact with DNA, however complexes **6**−**8** which contain the planar chelating phen ligand compete effectively with the EtBr (Figure 5) and have notable binding constants (Table 4). It is noteworthy that complex **7**, which contains the bulky 3,5-diispropylsalicylate anion, is the least competitive of the three phen derivatives and interacts less effectively with the DNA, which may result from a steric effect. Interestingly, **7** also displayed the lowest cytotoxic activity for three of the cancer cell lines over the 24 h exposure, suggesting that the relative binding strength of the complexes to DNA is an important element of the mode of action of these three compounds. Significantly "metal free" phen did not appear to reduce the fluorescence, suggesting it may not displace the DNA bound Et^+ in this experiment.

While the indirect fluorescence studies conducted with EtBr provide excellent analysis on the binding interactions of complexes **6**−**8**, in order to confirm if their interactions with the biomolecule involves intercalation, viscosity studies were carried out.[43,44] The DNA viscosity titrations were conducted using "metal free" phen, complexes **6**−**8**, and the known intercalator EtBr and known minor groove binding drug

dx.doi.org/10.1021/jm201041d | J. Med. Chem. 2012, 55, 1957−1968

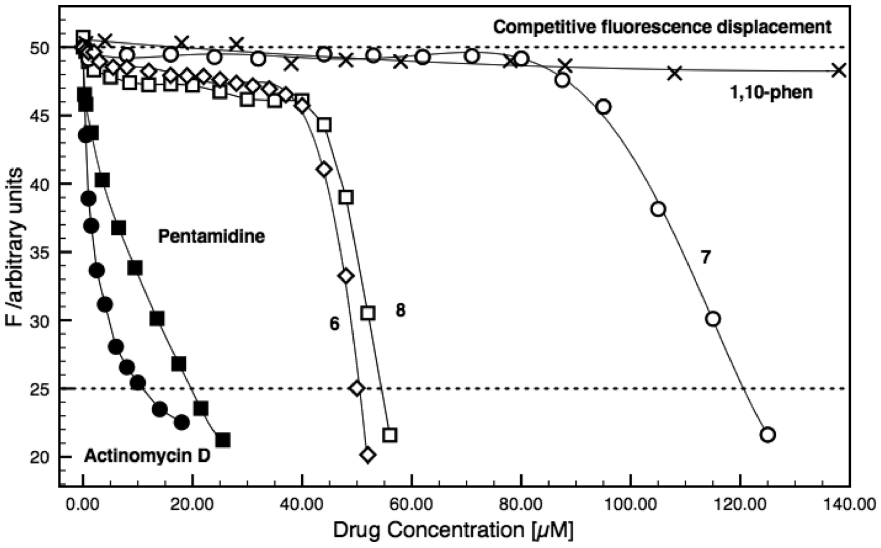

Figure 5. Competitive EtBr displacement for actinomycin D, pentamidine, "metal free" phen, and complexes **6**–**8** with Ct-DNA.

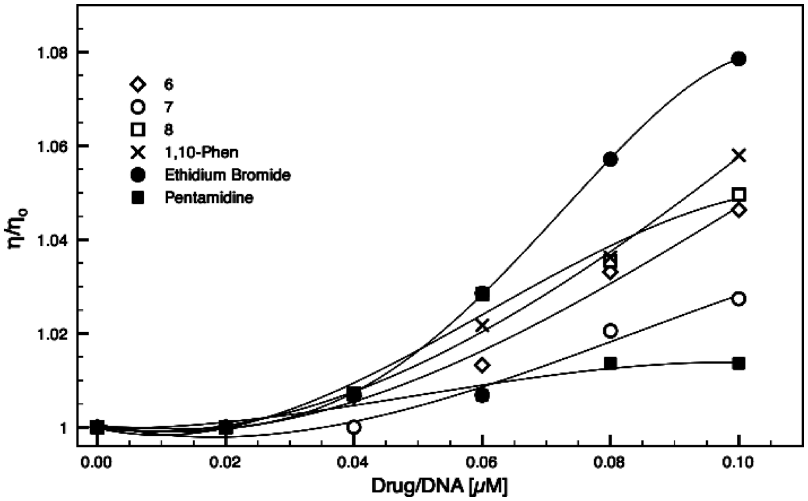

Figure 6. Relative viscosity increments of CT-DNA upon exposure to complexes **6**–**8**, metal-free 1,10-phen, ethidium bromide, and pentamidine. Data are reported as η/η_0 versus [compound]/[DNA] ratio, in which η and η_0 refer to the viscosity of each DNA working sample in the absence and presence of tested compound, respectively.

pentamidine as controls. As shown in Figure 6, with increasing [compound]/[DNA] ratios from 0.02 to 0.10, the DNA viscosity profiles of both EtBr and pentamidine are as expected for an intercalator and a minor groove binder, respectively.[43,44] In contrast to the fluorescence analysis above, the "metal free" phen exhibits a strong tendency to interact the DNA and its increasing viscosity profile suggests it is an effective intercalator. It should be noted that such strong DNA binding has been reported previously for similar phen derivatives.[45] Complexes **6** and **8** exhibit similar profiles of increasing viscosity to that of the "metal free" phen, again suggesting intercalation as their main binding mode with the CT-DNA. Complex **7** also exhibits a tendency of increasing viscosity which supports intercalation as a mode of interaction with DNA but it exerts less of an effect on the DNA viscosity than complexes **6** and **8**, which compares well with the indirect fluorescence studies above and again may result from the presence of the relatively bulky 3,5-diispropylsalicylate anion in its structure.

2.7. Nuclease Activity. The oxidative DNA cleavage activity of 1,10-phenanthroline in the presence of Cu^{2+} mediated by the coreactant H_2O_2 and added reductant was reported by Sigman et al. in 1979.[46] Since then, many copper containing complexes have been shown to oxidatively cleave DNA in the presence of added reductant and clearly this mimetic nuclease activity could contribute to the cytotoxic potency of such copper complexes. The DNA cleaving abilities of complexes **1**–**8** were investigated by reaction with supercoiled (SC) pUC18 DNA and the relative mobility of the products on agarose gel. SC DNA was exposed to **1**–**8** at concentrations of 50 and 25 μM for 2 h in the presence of added ascorbate at 37 °C (Figure 7).

At the 50 μM concentration (Figure 7a), complexes **1**–**5** show some ability to cleave SC (super coiled) (form I) DNA to OC (open circular) (form II). Of the two benzimidazole complexes (lanes 4 and 5), only complex **5** was capable of inducing complete relaxation of SC (form I) DNA to OC (form II). The phen containing complexes **6** and **8** were found to completely digest the DNA, as characterized by the absence of a band in lanes 6 and 8. Complex **7**, which has less affinity for DNA (Table 4), was capable of inducing relaxation of SC

dx.doi.org/10.1021/jm201041d | J. Med. Chem. 2012, 55, 1957–1968

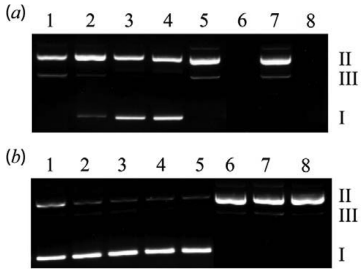

Figure 7. Relaxation of pUC18 DNA by complexes **1**–**8** at (a) 50 μM complex concentration, 2 h incubation in the presence of added ascorbate (at twice complex concentration), lanes 1–8, complexes **1**–**8**; (b) 25 μM complex concentration, 2 h incubation in the presence of added ascorbate (at twice complex concentration), lanes 1–8, complexes **1**–**8**.

(form I) DNA to OC (form II). At the lower concentration of 25 μM (Figure 7b), complexes **1**–**5** were incapable of causing relaxation of DNA, whereas the phen complexes **6**–**8** induced complete relaxation to OC (form II) DNA, (Figure 7b) lanes 6–8.

To further elucidate the observed activities of complexes **6**–**8**, a study of their nuclease capabilities across the concentration range 10, 20, 30, 40, and 50 μM was conducted over a prolonged exposure (5 h) to super coiled DNA (Supporting Information Figure S2). The results clearly indicate a concentration dependent effect on the conversion of SC DNA to first the OC form, followed by LC (linear conformation), with the bulkier 3,5-diispropylsalicylate containing complex (**7**), again being the least active of the three complexes. In the absence of added ascorbate, of the eight complexes only complexes **6** and **8** show any ability to relax closed circular DNA but only at a maximum concentration of 50 μM (Supporting Information Figure S3). Complex **7** is typical of the remaining six complexes which show no ability to interact with closed circular DNA in the absence of the added reductant. The interaction of **6** and **8** with SC DNA most likely represents a mechanical-type unwinding whereby at high complex load these intercalating species distort the conformation of the super helix, leading to the observed partial unwinding. This interaction is very different to the chemical (oxidative) scission, which occurs in the presence of added reductant.

In conclusion, the complexes which displayed the highest affinity for binding DNA (**6**–**8**) (Figure 5) were also the most efficient at inducing relaxation of the DNA molecule, and there is an interesting similarity between their observed in vitro nuclease activities and those seen in the cell-based cytotoxicity assays.

3. CONCLUSIONS

Our results show that the simple copper complexes of salicylic, 3,5-diisopropylsalicylic, and 3-methoxysalicylic acids are potent superoxide dismutase mimetics capable of catalytically scavenging the pro-inflammatory superoxide radical and that they are inactive as catalase mimetics. Addition of either monodentate benzimidazole or the chelating 1,10-phenanthroline ligands to these complexes does not improve their SOD activity or their ability to catalytically disproportionate H_2O_2. Despite the similarities in the superoxide dismutase mimetic activity of all eight complexes, they do not exhibit similar cytotoxic activity against the cisplatin sensitive and resistant cell lines tested. Over the 24 h exposure period the free ligands, the simple salicylate complexes **1**–**3** and the square planar benzimidazole derivatives **4** and **5** were essentially inactive against all four tumor cell lines. In contrast, the square planar bis-chelate (salicylate^{2-}/phen) complexes **6**–**8** exhibited rapid low-micromolar cytotoxicity against both the cisplatin sensitive and resistant cancer cells. The complexes are all inactive as inhibitors of COX-2 activity with the nonchelated complexes **1**, **4**, and **5**, exhibiting only marginal to moderate inhibition of COX-1, suggesting that interference in the arachidonic acid cascade is not part of the mode of action of the highly cytotoxic bis-chelate (salicylate^{2-}/phen) complexes **6**, **7**, and **8**. Significantly, of the eight complexes, only these phen derivatives were capable of binding to DNA as intercalators with complex **7**, which contains the bulky 3,5-diispropylsalicylate anion, interacting least effectively with the biomolecule. Interestingly, **7** also displayed the lowest cytotoxic activity for three of the cancer cell lines over 24 h, suggesting that the relative binding strength of the complexes to DNA may be an important element of the mode of action of these three compounds. Complexes **6**–**8** were also the most efficient at inducing relaxation of the DNA molecule, and there is an interesting similarity between their observed in vitro nuclease activities and those seen in the cell-based cytotoxicity assays.

In conclusion, the results obtained from this study show that the bis-chelate [Cu^{2+}(salicylate)$^{2-}$(phen)] complexes could be valuable tools in cancer chemotherapy and further studies into their mode of action are currently underway.

4. EXPERIMENTAL SECTION

Chemicals and CT-DNA were purchased from Sigma Aldrich (Ireland) and used without further purification. Supercoiled plasmid DNA (pUC18) was supplied by Roche Diagnostics Ltd. (UK). The COX inhibitory screening assay was supplied by Cayman Chemicals (USA). Solid-state IR were recorded in the region 4000–400 cm^{-1} on a Nicolet FT-IR 5DXB infrared spectrometer, with solid samples first being finely ground then mixed with KBr. Pellets consisted of 5 mg of analyte per 195 mg of KBr. Magnetic susceptibility measurements were made using a Johnson Matthey magnetic susceptibility balance. [$HgCo(SCN)_4$] was used as a reference. UV–vis spectra were recorded in both solution and solid state using a Varian Cary 50 Scan single beam spectrophotometer which covered the range 800–190 nm using a Xenon lamp as the light source. Solid-state samples were generated by finely grinding samples of each complex and then drop-casting from a chloroform suspension onto a glass substrate. Solution-state spectra were recorded at 4.0 mM in DMSO. Molar conductivity measurements were made at 25 °C using an Orion 150 Aplus conductivity meter at 4.0 mM in DMSO. Viscosity experiments were carried out using an A&D SV-10 viscometer. Elemental analytical data for the complexes were reported by the Microanalytical Laboratory, University College Dublin, Ireland, and the Microanalytical Laboratory, University College Cork, Ireland.

4.1. Synthesis of the Compounds. [$Cu(salH)_2(H_2O)_2$] (**1**) and [Cu(sal)(phen)]·H_2O (**6**) were synthesized and characterized using methods previously published.[23,24]

[$Cu(dipsH)_2(H_2O)$] (**2**) and {$Cu(3\text{-}MeOsal)(H_2O)_{0.75}\}_n$ (**3**) were obtained, as green and brown powders respectively, by refluxing a suspension of 5 mmol of $Cu(OH)_2$ and 10 mmol of the respective salicylic acid in EtOH (75 mL) for 3 h. On cooling to room temperature, the product was filtered off, washed with two portions of water and ethanol, and then air-dried. [$Cu(dipsH)_2(H_2O)$] (**2**): Yield, 2.86 g (54%). Percent calcd: C, 59.58; H, 6.92. Percent found: C, 59.27; H, 6.83. IR (KBr): 3432, 2961, 2930, 2870, 1807, 1628, 1592, 1560, 1468, 1390, 1363, 1319, 1296, 1241, 1175, 1151, 1123, 1107, 1084, 1046, 944, 895, 877, 844, 808, 780, 741, 702, 639, 573, 536, 470 cm^{-1}. Solubility: DMSO, EtOH. μ_{eff}: 1.38 μ_B λ_{max}(Nujol): λ_{d-d} = 703

dx.doi.org/10.1021/jm201041d | J. Med. Chem. 2012, 55, 1957–1968

Table 5. Details of the Crystal Data Collection and Refinement for 4, 5, and 8

	4	5	8
empirical formula	$C_{40}H_{46}CuN_4O_6$	$C_{46}H_{62}CuN_4O_{10}$	$C_{40}H_{32}Cu_2N_4O_{10}$
formula wt	742.35	894.55	855.78
crystal system	triclinic	monoclinic	monoclinic
space group	$P\bar{1}$	$P2(1)/n$	$P2(1)/c$
a (Å)	6.1772(5)	14.1585(16)	9.1568(8)
b (Å)	8.5643(7)	9.4205(11)	16.7752(16)
c (Å)	17.7321(12)	17.5813(17)	11.8598(11)
α (deg)	90.019(3)	90	90
β (deg)	87.088(3)	101.756(3)	108.185(4)
γ (deg)	81.686(4)	90	90
vol (Å^3)	927.00(12)	2295.8(4)	1730.8(3)
Z	1	2	2
density (calcd) (mg/m^3)	1.330	1.294	1.642
absorption coefficient (mm^{-1})	0.641	0.536	1.299
F(000)	391	950	876
crystal size (mm^3)	0.56 × 0.14 × 0.12	0.46 × 0.22 × 0.20	0.44 × 0.10 × 0.08
θ range for data collection (deg)	2.30−32.29	2.46−32.58	2.64−26.39
reflections collected	22939	57302	34510
independent reflections	5801 [R(int) 0.0281]	7682 [R(int) 0.0503]	3492 [R(int) = 0.0602]
completeness to θ = 25.00° (%)	97.7	99.3	99.9
max and min transmission	0.9270 and 0.7154	0.898 and 0.782	0.901 and 0.723
data/restraints/parameters	5801/1/240	7682/0/290	3492/3/262
goodness-of-fit on F^2	1.036	0.988	1.010
final R indices [$I > 2\sigma(I)$]: $R1$, $wR2$	0.0355, 0.0864	0.0455, 0.1139	0.0443, 0.1123
R indices (all data) $R1$, $wR2$	0.0483, 0.0923	0.0745, 0.1282	0.0661, 0.1263
largest diff. peak and hole (e·Å^{-3})	0.440 and −0.408	0.743 and −0.622	0.504 and −0.684

nm λ_{max}(DMSO): λ_{d-d} = 766 nm, ε = 113.26 dm^3 mol^{-1} cm^{-1}. Λ_M(DMSO): 9.3 S cm^2 mol^{-1}. {Cu(3-MeOsal)$(H_2O)_{0.75}$}$_n$ (**3**): Yield: 2.0283 g (81%). Percent calcd: C, 39.50; H, 3.08. Percent found: C, 39.75; H, 2.85. IR (KBr): 3431, 2940, 2840, 1633, 1606, 1588, 1533, 1473, 1450, 1402, 1247, 1207, 1163, 1088, 1061, 934, 856, 835, 812, 779, 753, 696, 644, 465 cm^{-1}. Solubility: insoluble. μ_{eff}: 1.65 μ_B λ_{max}(Nujol): λ_{d-d} = 764 nm.

[Cu(dipsH)$_2$(BZDH)$_2$] (**4**) and [Cu(dipsH)$_2$(2-MeOHBZDH)$_2$]·EtOH (**5**) were obtained, as blue powders, by refluxing a solution of 0.76 mmol of [Cu(dipsH)$_2$(H$_2$O)] (**2**) with 1.52 mmol of the respective benzimidazole in EtOH (75 mL) for 3 h. On cooling to room temperature, the product precipitated and was filtered off, washed with two portions of water and ethanol, and then air-dried. [Cu(dipsH)$_2$(BZDH)$_2$] (**4**): Yield, 0.36 g (55%). Percent calcd: C, 64.72; H, 6.25; N, 7.55. Percent found: C, 64.36; H, 6.23; N, 7.33. IR (KBr): 3427, 3139, 3031, 2959, 2926, 2867, 1807, 1618, 1590, 1550, 1500, 1466, 1458, 1487, 1405, 1362, 1315, 1303, 1267, 1245, 1176, 1154, 1141, 1126, 1112, 1085, 1070.1009, 965.943, 896, 8884, 845, 814, 774, 753, 746, 660, 640, 634, 620, 577, 549, 527, 503, 460, 449, 423 cm^{-1}. Solubility: DMSO. μ_{eff}: 1.69 μ_B λ_{max}(Nujol): λ_{d-d} = 563 nm. λ_{max}(DMSO): λ_{d-d} = 733 nm, ε = 81.95 dm^3 mol^{-1} cm^{-1}. Λ_M(DMSO): 18.65 S cm^2 mol^{-1}. [Cu(dipsH)$_2$(2-MeOHBZDH)$_2$]·EtOH (**5**): Yield, 0.31 g (47%). IR (KBr): 3425, 3115, 3067, 2961, 2927, 2869, 1620, 1553, 1469, 1457, 1388, 1362, 1329, 1292, 1242, 1175, 1151, 1122, 1106, 1079, 1043, 1005, 920, 894, 812, 776, 744, 640, 575, 540, 492, 429 cm^{-1}. Solubility: DMSO. μ_{eff}: 1.79 μ_B λ_{max}(Nujol): λ_{d-d} = 575 nm. λ_{max}(DMSO): λ_{d-d} = 740 nm, ε = 44.18 dm^3 mol^{-1} cm^{-1}. Λ_M(DMSO): 5.15 S cm^2 mol^{-1}. A small quantity of blue crystals of **4** and **5**, suitable for X-ray structural analysis, were obtained from the respective filtrates upon standing for one week.

[Cu(dips)(phen)]·H$_2$O (**7**) and [Cu(3-MeOsal)(phen)]·H$_2$O (**8**) were obtained, as green powders, by refluxing a suspension of 1.3 mmol of either **2** or **3** with 2.6 mmol of phen in EtOH (75 mL) for 3 h. On cooling to room temperature, the product was filtered off, washed with two portions of water and ethanol, and then air-dried. [Cu(dips)(phen)]·H$_2$O (**7**): Yield, 0.54 g (86%). Percent calcd: C, 62.03; H, 5.83; N, 5.80. Percent found: C, 62.48; H, 5.86; N, 5.87. IR (KBr): 3431, 3075, 3055, 2952, 2864, 1807, 1628, 1612, 1575, 1548, 1516, 1491, 1467, 1454, 1427, 1369, 1344, 1312, 1284, 1241, 1223, 1174, 1148, 1107, 1047, 972, 944, 921, 893, 873, 845, 815, 802, 751, 737, 724, 685, 646, 634, 578, 542, 432, 421 cm^{-1}. Solubility: DMSO. μ_{eff}: 2.05 μ_B λ_{max}(Nujol): λ_{d-d} = 631 nm. λ_{max}(DMSO): λ_{d-d} = 644 nm, ε = 67.31 dm^3 mol^{-1} cm^{-1}. Λ_M(DMSO): 0.78 S cm^2 mol^{-1}. [Cu(3-MeOsal)(phen)]·H$_2$O (**8**): Yield, 0.55 g (64%). Percent calcd: C, 56.14; H, 3.77; N, 6.55. Percent found: C, 56.09; H, 3.41; N, 6.14. IR (KBr): 3432, 3059, 2835, 1630, 1568, 1572, 1554, 1519, 1472, 1445, 1429, 1369, 1340, 1234, 1199, 1147, 1108, 1063, 923, 874, 847, 821, 800, 751, 736, 722, 674, 627, 566, 453, 432 cm^{-1}. Solubility: DMSO. μ_{eff}: 1.85 μ_B λ_{max}(Nujol): λ_{d-d} = 602 nm. λ_{max}(DMSO): λ_{d-d} = 640 nm, ε = 273.8 dm^3 mol^{-1} cm^{-1}. Λ_M(DMSO): 1.45 S cm^2 mol^{-1}. A small quantity of green crystals of **8**, suitable for X-ray structural analysis, were obtained from the filtrate upon standing for one week.

Note: The elemental analysis results for complexes **1**, **2**, **3**, **4**, **6**, and **8** confirm that the purity of the isolated compounds is ≥95%. The elemental analytical results for complex **5** have not been included as difficulty removing the solvent of crystallization disabled the elemental analysis of this particular compound. The elemental analytical results for complex **7** are consistent with the loss of a very small amount of water of crystallization prior to analysis.

4.2. X-Ray Crystallography. Data for **4**, **5**, and **8** were collected at 100K on a Bruker X8 APEXII CCD system[47] with Mo Kα radiation (λ = 0.7107 Å). The structures were solved by direct methods, and all non H atoms were refined anisotropically against F^2 using SHELXS and SHELXL-97.[48] All N-bound Hydrogen atoms were located in the difference Fourier map and in **4** N−H distances were restrained [0.89 (2) Å] as were the water H atoms in **8** O−H [0.90(2) Å] and H···H [1.50 (4) Å]. Hydroxyl H atoms were placed in calculated positions and constrained to ideal geometry, but in **4** the hydroxyl H bound to O4 was located in the difference Fourier map and refined freely. All other H atoms were constrained to idealized geometries. Isotropic thermal parameters of all H atoms were fixed to 1.2 times (1.5 times for methyl and hydroxyl) the equivalent isotropic thermal parameter of their parent atoms Table S summarizes the crystallographic data for these compounds.

dx.doi.org/10.1021/jm201041d | J. Med. Chem. 2012, 55, 1957−1968

4.3. Cytotoxicity Assays. The cytotoxic potential of the free ligands, a simple copper salt, complexes **1**−**8** along with cisplatin, was determined following incubation of exponentially growing cells using the MTT assay[49] at the Centre of Applied Science for Health, ITTD, Dublin, Ireland. Human breast cancer cell line, MCF-7 (passage 16−26, ATCC, USA), was grown in Eagle's Minimum Essential Medium (EMEM) containing 2 mM L-glutamine, penicillin−streptomycin solution with 100 U/mL penicillin and 100 μg of streptomycin per mL, FBS (10%), sodium pyruvate (1 mM), and 1% (v/v), nonessential amino acid solution. Human prostate cancer cell line, DU145 (passage 12−29, ATCC, USA) was grown in EMEM containing 2 mM L-glutamine, penicillin−streptomycin solution with 100U/ml penicillin and 100 μg of streptomycin per mL, 10% FBS, sodium pyruvate (1 mM) and 1% (v/v), and nonessential amino acid solution. Human ovarian cell line, SKOV-3 (passage 56−61) were grown in McCoys 5A medium supplemented with 2 mM glutamine and 10% FBS and containing 100 U/mL penicillin and 100 μg of streptomycin per mL. Human colon cancer cell line, HT29 (passage 17 to 30, ATCC, USA), was grown in McCoys's 5a Medium supplemented with 2 mM L-glutamine and 10% FBS and containing penicillin−streptomycin solution with 100 U/mL penicillin and 100 μg of streptomycin per mL. All four cell lines were maintained at 37 °C in a humidified atmosphere with 5% CO_2. All drugs were tested by MTT assay following either 24 h or 96 h exposure of cells to each compound. The MTT assay was carried out by seeding cells at 4×10^5 cells/mL in 96-well plates and incubated at 37 °C in 5% CO_2 for 24 h. Cells were treated with a four log range of concentrations of the test compounds in triplicate from 0.1 to 100 μM or with a solvent control (0.5% DMSO) in complete medium. Following 24 or 96 h incubation, cells were incubated with 20 μL of MTT (5 mg/mL) in 0.1 M PBS, pH 7.4, at 37 °C in a humid atmosphere with 5% CO_2 for 4 h. Media was then gently aspirated from test cultures, and 100 μL of dimethyl sulfoxide (DMSO) was added to all wells. The plates were then shaken for 2 min, and the absorbance was read at 550 nm in a Varioscan plate reader. The IC_{50} was defined as the concentration of test compound required to reduce the absorbance of the MTT-formazan crystals by 50%, indicating a 50% reduction in cell viability. Each value represents the mean IC_{50} of three separate experiments. IC_{50} values were derived as follows: The individual graphs for three individual experiments carried out on a given complex in a specific cell line were plotted separately by plotting the % viability against concentration, analyzed by nonlinear regression, and the IC_{50} values for each individual experiment was determined at the concentration where the viability was 50% of untreated control. The mean of three individual IC_{50} values were then obtained and are reported as the mean ± standard error of the mean (±SEM). The IC_{50} values are all relative to the vehicle control. Maximal inhibition varied from >50% to <0.1% depending on the complex being tested and was limited at the top concentration used (100 μM in all cases).

4.4. Superoxide Dismutase (SOD) Activity. The $O_2^{\bullet-}$ dismutase activities of the metal complexes were assessed using a modified Nitro-Blue-Tetrazolium (NBT) assay with xanthine−xanthine oxidase system as the source of $O_2^{\bullet-}$.[50] The quantitative reduction of NBT to blue Formazan by the $O_2^{\bullet-}$ was followed spectrophotometrically at 550 nm. All reagents were obtained from Sigma-Aldrich Chemical Co. Ltd., and assays were run in 3 mL of solution. Results are graphed as the % inhibition of NBT reduction for three concentrations. Tabulated results were derived from linear regression analyses and are given as the concentration (μM) equivalent to 1 unit of bovine erythrocyte SOD activity. A unit SOD activity is the concentration of the complex or enzyme which causes 50% inhibition in the reduction of NBT (referred to as the IC_{50} value).

4.5. Inhibition of COX Enzymes. The inhibition of isolated ovine COX-1 and human recombinant COX-2 at 10 μM concentrations of free salicylic acid and the respective complexes was determined by ELISA (COX Inhibitory Screening Assay; Cayman Chemical Company, Ann Arbor, MI). The experiments were performed according to the manufacturers instructions. The principal behind the COX assay is based on a competition between free prostaglandin (PG) (specifically PGH_2), which is produced by COX enzyme activity, and a prostaglandin conjugate, which acts as the COX assay tracer (PG-acetylcholinesterase) for a limited amount of prostaglandin rabbit antiserum which in turn binds specifically to a mouse monoclonal antirabbit antibody attached to the wells of a prepared 96 well plate. The concentration of the PG tracer is held constant compared to the free PG, and therefore the amount of PG tracer that can bind to the PG rabbit antiserum is inversely proportional to the concentration of PG in the well. Normal COX-1 or COX-2 enzyme activity will show high levels of free PG production compared to the PG tracer (as measured by absorbance at 405 nm). Inhibition of COX-1 or COX-2 enzyme activity will show lower levels of free PG being produced when compared to the PG tracer.

4.6. DNA−Copper Complex Interaction Studies. A working solution containing 1 μM CT-DNA (ε_{260} = 12,824 $M(bp)^{-1}$ cm^{-1}) along with 1.26 μM ethidium bromide (EtBr) at neutral pH in TES buffer (10 mM TES, 0.1 mM Na_2EDTA, pH = 7.0) was prepared. Complexes **1**−**8**, actinomycin D, pentamidine isothionate, Cu(II) nitrate, and phen were prepared at 2.0 mM in DMSO. Two milliliters of DNA-Et solution were placed in a 10 mm quartz cuvette (3 mL) and positioned in a temperature controlled (20 °C) spectrofluorometer (Perkin-Elmer LS55B luminescence spectrometer). Excitation and emission wavelengths were set to 546 and 595 nm, respectively. After thermal equilibrium was established, the emission and excitation slits were modified to give a fluorescence reading of 50 arbitrary units, with measurements being recorded over a 20 s interval. An aliquot of complex or drug solution was taken (0.5−10 μL) and added to the cuvette, and after equilibration the fluorescence reading was recorded. Repeated aliquots were added until the fluorescence was 20−40% of the initial control. Triplicate titrations were performed and the apparent binding constants were calculated using $K_{app} = K_e \times 1.26/C_{50}$ where $K_e = 9.5 \times 10^6$ $M(bp)^{-1}$ (K_{app} = apparent binding constant).

4.7. Viscosity Experiments. Ten mL of CT-DNA solution was prepared at 1 mM in TES buffer (10 mM TES, 0.1 mM Na_2EDTA, pH = 7.0) for each working sample. Complexes **6**−**8**, ethidium bromide, actinomycin D, and 1,10-phen were prepared at 4 mM in DMSO. Stock solutions of compound were added according to the increasing [compound]/[DNA] ratios of 0.02, 0.04, 0.06, 0.08, and 0.10 and their viscosity measured. Temperature was maintained at 25 °C. Data were presented as η/η_0 versus [compound]/[DNA] ratio, in which η and η_0 refers to the viscosity of each DNA working sample in the absence and presence of compound respectively.

4.8. DNA Cleavage. Reactions were carried out in a total volume of 15 μL using 20 mM sodium phosphate buffer (pH = 7.2), 20 mM NaCl, 25 or 50 μM of complexes **1**−**8** (prepared in DMF), sodium-L-ascorbate (at twice the complex concentation) along with 0.75 μL of 0.25 μg/μL pUC18 (Roche). Samples were incubated for 5 h at 37 °C. Quench buffer (3 μL; 0.25% bromophenolblue, 0.25% xylene cyanole, and 30% glycerol) was then added, and samples were loaded onto agarose gel (1%) containing 1.5 μL of GelRed (10000×). Electrophoresis was completed at 80 V for 2 h in 1× TAE buffer. Additional DNA cleavage experiments were conducted (Supporting Information) which studied (i) the interaction of complexes **6**−**8** with DNA across the concentration range 10, 20, 30, 40, and 50 μM (Supporting Information Figure S2) and (ii) the interaction of complexes **6**−**8** across the concentration range 10, 20, 30, 40, and 50 μM in the absence of added ascorbate (Supporting Information Figure S3)

■ ASSOCIATED CONTENT

Ⓢ Supporting Information

Hydrogen peroxide disproportionation data, representative cytotoxicy plots, and additional DNA nuclease data. This material is available free of charge via the Internet at http://pubs.acs.org. CIF files for compounds **4**, **5**, and **8** have been deposited with the Cambridge Crystallographic Data Centre (CCDC 804688, 804689, and 804690, respectively).

AUTHOR INFORMATION

Corresponding Author

*Phone: +353 1 4024585. Fax: +353 1 4024998. E-mail: Michael.Devereux@dit.ie. Address: College of Sciences and Health, Dublin Institute of Technology, Kevin Street, Dublin 8, Ireland.

Present Addresses

[⊥]Chemistry Department, National University of Ireland, Maynooth, County Kildare, Ireland.

[#]School of Chemical Sciences and the National Institute for Cellular Biotechnology, Dublin City University, Glasnevin, Dublin 9, Ireland.

Notes

The authors declare no competing financial interest.

ACKNOWLEDGMENTS

We acknowledge financial support from the Irish Technological Sector Research Strand I and Strand III programmes (project nos. PT03147 and CRS02-TA01, respectively) and from the Dublin Institute of Technology Capacity Building Scheme for Strategic Research progamme (CaBS). This work has been carried out (in part) within the structures of the Facility for Optical Characterisation and Spectroscopy (now the FOCAS Institute, DIT), funded under The Irish National Development Plan 2000−2006 with assistance from the European Regional Development Fund.

ABBREVIATIONS USED

BM, Bohr magneton; BZDH, benzimidazole; COX, cyclooxygenase; CT-DNA, calf thymus DNA; CuZnSOD, copper−zinc superoxide dismutase; dipsH_2, 3,5-diisopropylsalicylic acid; DMSO, dimethylsulfoxide; EDTA, ethylenediaminetetraacetic acid; EtBr, ethidium bromide; EtOH, ethanol; IC_{50}, concentration required for 50% inhibition; indoH, indomethacin; K_{app}, apparent binding constant; MeOH, methanol; 2-MeOHBZDH, 2-methanolbenzimidazole; 3-MeOsalH_2, 3-methoxysalicylic acid; MnSOD, manganese superoxide dismutase; NBT, nitroblue-tetrazolium; NSAID, nonsteroidal anti-inflammatory drug; OAc, acetate; OC, open circular; odaH_2, octanedioic acid; phen, 1,10-phenanthroline; phendione, 1,10-phenanthroline-5,6-dione; PGH_2, prostaglandin; ROS, reactive oxygen species; salH_2, salicylic acid; sal^{2-}, salicylate dianion; SC, supercoiled; SOD, superoxide dismutase

REFERENCES

(1) Coussens, L. M.; Werb, Z. Inflammation and cancer. *Nature* **2002**, *420*, 860−867.

(2) Dvorak, H. F. Tumors: wounds that do not heal. *N. Engl. J. Med.* **1986**, *315*, 1650−1659.

(3) Mantovani1, A.; Allavena1, P.; Sica, A.; Balkwill, F. Cancer-related inflammation. *Nature* **2008**, *454*, 436−444.

(4) Fridovich, I. Fundamental aspects of reactive oxygen species or what's the matter with oxygen? *Ann. N.Y. Acad. Sci.* **1999**, *893*, 13−18.

(5) Muscoli, C.; Cuzzocrea, S.; Riley, D. P.; Zweier, J. L.; Thiemermann, C.; Wang, Z. Q.; Salvemini, D. On the selectivity of superoxide dismutase mimetics and its importance in pharmacological studies. *Br. J. Pharmacol.* **2003**, *140*, 445−460.

(6) Huang, P.; Feng, L.; Oldam, E. A.; Keating, M. J.; Plunkett, W. Superoxide dismutase as a target for the selective killing of cancer cells. *Nature* **2000**, *407*, 390−395.

(7) Oberley, L. W. Anticancer therapy by overexpression of superoxide dismutase. *Antioxid. Redox Signaling* **2001**, *3*, 461−472.

(8) Salvemini, D.; Doyle, T. M.; Cuzzocrea, S. Superoxide, peroxynitrite and oxidative/nitrative stress in inflammation. *Biochem. Soc. Trans.* **2006**, *34*, 965−970.

(9) Salvemini, D.; Riley, D. P.; Cuzzocrea, S. SOD mimetics are coming of age. *Nature Rev. Drug Discovery* **2002**, *1*, 367−374.

(10) Darby Weydert, C. J.; Smith, B. B.; Xu, L.; Kregel, K. C.; Ritchie, J. M.; Davis, C. S.; Oberley, L. W. Inhibition of oral cancer cell growth by adenovirus *MnSOD* plus BCNU treatment. *Free Radical Biol. Med.* **2003**, *34*, 316−329.

(11) Lam, E. W. N.; Hammand, H. M.; Zwacka, R.; Darby, C. J.; Baumgardner, K. R.; Davidson, B. L.; Oberley, T. D.; Engelhardt, J. F.; Oberley, L. W. Adenovirus-mediated manganese superoxide dismutase gene transfer to hamster cheek pouch carcinoma cells. *Cancer Res.* **1997**, *57*, 5550−5556.

(12) Weydert, C. J.; Waugh, T. A.; Ritchie, J. M.; Iyer, K. S.; Smith, J. L.; Li, L.; Spitz, D. R.; Oberley, L. W. Overexpression of manganese or copper−zinc superoxide dismutase inhibits breast cancer growth. *Free Radical Biol. Med.* **2006**, *41*, 226−237.

(13) Weder, J. E.; Dillon, C. T.; Hambley, T. W.; Kennedy, B. J.; Lay, P. A.; Biffin, J. R.; Regtop, H. L.; Davies, N. M. Copper complexes of non-steroidal anti-inflammatory drugs: an opportunity yet to be realized. *Coord. Chem. Rev.* **2002**, *232*, 95−126.

(14) Huang, R.; Wallqvist, A.; Covell, D. G. Anticancer metal compounds in NCI's tumor screening database: putative mode of action. *Biochem. Pharmacol.* **2005**, *69*, 1009−1039.

(15) Vane, J. R.; Botting, R. M. Mechanism of action of anti-inflammatory drugs. *Int. J. Tissue React.* **1998**, *20*, 3−15.

(16) Dannhardt, G.; Kiefer, W. Cyclooxygenase inhibitors—current status and future prospects. *Eur. J. Med. Chem.* **2001**, *36*, 109−126.

(17) van Rijt, S. H.; Sadler, P. J. Current applications and future potential for bioinorganic chemistry in the development of anticancer drugs. *Drug Discovery Today* **2009**, *14*, 1089−1097.

(18) Garcia-Rodriguez, L. A.; Huerta-Alvarez, C. Reduced risk of colorectal cancer among long-term users of aspirin and non-aspirin nonsteroidal anti-inflammatory drugs. *Epidemiology* **2001**, *12*, 88−93.

(19) Ulrich, C. M.; Bigler, J.; Potter, J. D. Nonsteroidal anti-inflammatory drugs for cancer prevention: promise, perils and pharmacogenetics. *Nature Rev. Cancer* **2006**, *6*, 130−140.

(20) Sorenson, J. R. J. Copper chelates as possible active forms of the antiarthritic agents. *J. Med. Chem.* **1976**, *19*, 135−148.

(21) Beveridge, S. J.; Walker, W. R.; Whitehouse, M. W. Anti-inflammatory activity of copper salicylates applied to rats precutaneously in dimethyl sulphoxide with glycerol. *J. Pharm. Pharmacol.* **1980**, *32*, 425−427.

(22) Sorenson, J. R. J.; Oberley, L. W. Copper complexes for treating cancer. U.S. Patent US4952607, 1990; http://www.freepatentsonline.com/4952607.html .

(23) Devereux, M.; O'Shea, D.; O'Connor, M.; Grehan, H.; Connor, G.; McCann, M.; Rosair, G.; Lyng, F.; Kellett, A.; Walsh, M.; Egan, D.; Thati, B. Synthesis, catalase, superoxide dismutase and antitumour activities of copper(II) carboxylate complexes incorporating benzimidazole, 1,10-phenanthroline and bipyridine ligands: X-ray crystal structures of $[Cu(BZA)_2(bipy)(H_2O)]$, $[Cu(SalH)_2(BZDH)_2]$ and $[Cu(CH_3COO)_2(5,6\text{-DMBZDH})_2]$ ($SalH_2$ = salicylic acid; BZAH = benzoic acid; BZDH = benzimidazole and 5,6-DMBZDH = 5,6-dimethylbenzimidazole). *Polyhedron* **2007**, *26*, 4073−4084.

(24) Geraghty, M; Sheridan, V.; McCann, M.; Deveruex, M.; McKee, V. Synthesis and anti-*Candida* activity of copper(II) and manganese-(II) carboxylate complexes X-ray crystal structures of $[Cu(sal)(bipy)]\cdot C_2H_5OH\cdot H_2O$ and $[Cu(norb)(phen)_2]\cdot 6.5H_2O$ ($salH_2$ = salicylic acid; $norbH_2$ = *cis*-5-norbornene-*endo*-2,3-dicarboxylic acid; bipy = 2,2′-bipyridine; phen = 1,10-phenanthroline). *Polyhedron* **1999**, *18*, 2931−2939.

(25) Hanic, V. F.; Michalov, J. Die Kristallstruktur von Kupfersalicylat-Tetrahydrat $Cu(OH.C_6H_4\cdot COO)_2\cdot 4H_2O$. *Acta Crystallogr.* **1960**, *13*, 299−302.

(26) Devereux, M.; McCann, M.; Casey, M.; Curran, M.; Ferguson, G.; Cardin, C.; Convery, M.; Quillet, V. Binuclear and Polymeric Manganese(II) Salicylate Complexes: Synthesis, Crystal Structure and

Catalytic Activity of $[Mn_2(Hsal)_4(H_2O)_4]$ and $[\{Mn_2(sal)_2(Hsal)(H_2O)(H_3O)(py)_4\cdot 2py\}_n]$ (H_2sal = salicylic acid, py = pyridine). *J. Chem. Soc., Dalton Trans.* **1995**, 771−776.

(27) Nakamoto, K., in *Infrared and Raman Spectra of Inorganic and Coordination Compounds*, 5th ed., Part B; John Wiley & Sons: New York, 1997; p 54.

(28) Cotton, F. A.; Wilkinson, G., In *Advanced Inorganic Chemistry*, 6th ed.; Wiley: New York, 1999; p 867.

(29) Casey, M.; McCann, M.; Devereux, M.; Curran, M.; Cardin, C.; Convery, M.; Quillet, V.; Harding, C. Synthesis and structure of the $Mn^{II,II}$ complex salt $[Mn_2(\eta^1\eta^1\mu_2$ oda$)(phen)_4(H_2O)_2][Mn_2(\eta^1\eta^1\mu_2$-oda$)(phen)_4(\eta^1$-oda$)_2]\cdot 4H_2O$ (odaH$_2$= octanedioic acid): a catalyst for H_2O_2 disproportionation. *J. Chem. Soc., Chem. Commun.* **1994**, 2643−2645.

(30) Rosenberg, B. Platinum coordination complexes in cancer chemotherapy. *Naturwissenschaften* **1973**, *60*, 399−406.

(31) Zoroddu, M. A.; Zanetti, S.; Pogni, R.; Basosi, R. An electron spin resonance study and antimicrobial activity of copper(II)-phenanthroline complexes. *J. Inorg. Biochem.* **1996**, *63*, 291−300.

(32) Sun, Y. Induction of glutathione synthetase by 1,10-phenanthroline. *FEBS Lett.* **1997**, *408*, 16−20.

(33) Devereux, M.; O'Shea, D.; Kellett, A.; McCann, M.; Walsh, M.; Egan, D.; Deegan, D.; Kedziora, K.; Rosair, G.; Muller-Bunz, H. Synthesis, X-ray crystal structures and biomimetic and anticancer activities of novel copper(II)benzoate complexes incorporating 2-(4-thiazolyl)benzimidazole (thiabendazole), 2-(2-pyridyl)benzimidazole and 1,10-phenanthroline as chelating nitrogen donor ligands. *J. Inorg. Biochem.* **2007**, *101*, 881−892.

(34) Deegan, C.; McCann, M.; Devereux, M.; Coyle, B.; Egan, D. In vitro cancer chemotherapeutic activity of 1,10-phenanthroline (phen), $[Ag_2(phen)_3(mal)]\cdot 2H_2O$, $[Cu(phen)_2(mal)]\cdot 2H_2O$ and $[Mn(phen)_2(mal)]\cdot 2H_2O$ (malH$_2$ = malonic acid) using human cancer cells. *Cancer Lett.* **2007**, *247*, 224−233.

(35) Mc Bryde, W. A. E.; Brisbin, D. A.; Irving, H. The stability of metal complexes of 1,10-phenanthroline and its analogues. Part III. 5-Methyl-1,10-phenanthroline. *J. Chem. Soc.* **1962**, 5245−5253.

(36) Irving, H.; Mellor, D. H. The stability of metal complexes of 1,10-phenanthroline and its analogues. Part I. 1,10-Phenanthroline and 2,2′-bipyridyl. *J. Chem. Soc.* **1962**, 5222−5237.

(37) Weser, U.; Sellenger, K. H.; Lengfelder, E. W.; Werner; Strahle, J. Structure of Cu_2(indomethacin)$_4$ and the reaction with superoxide in aprotic systems. *Biochim. Biophys. Acta* **1980**, *631*, 232−245.

(38) In *IVS Annual*; MIMS Publishing: Crows Nest, Sydney, NSW, 1997; pp 145−276.

(39) Kaiser, J.; Csonka, R.; Speier, G.; Giorgi, M.; Reglier, M. Synthesis, structure and catalase-like activity of new dicopper(II) complexes with phenylglyoxylate and benzoate ligands. *J. Mol. Catal. A: Chem.* **2005**, *236*, 12−17.

(40) Kaiser, J.; Csay, T.; Speier, G.; Reglier, M.; Giorgi, M. Synthesis, structure and catalase-like activity of Cu(*N*-baa)$_2$(phen) (phen = 1,10 phenanthroline, *N*-baaH = *N* benzoylanthranilic acid). *Inorg. Chem. Commun.* **2006**, *9*, 1037−1039.

(41) Loll, P. J.; Picot, D.; Garvito, R. M. The structure basis for asprin activity inferred from the crystal structure of inactivated prostaglandinH$_2$ synthase. *Nature Struct. Biol.* **1995**, *2*, 637−643.

(42) Bruijnincx, P.; Sadler, P. J. New trends for metal complexes with anticancer activity. *Curr. Opin. Chem. Biol.* **2008**, *12*, 197−206.

(43) Satyanarayana, S.; Dabrowiak, J. C.; Chaires, J. B. Neither .DELTA.- nor .LAMBDA.-tris(phenanthroline)ruthenium(II) binds to DNA by classical intercalation. *Biochemistry* **1992**, *31* (39), 9319−9324.

(44) Satyanarayana, S.; Dabrowiak, J. C.; Chaires, J. B. Tris(phenanthroline)ruthenium(II) enantiomer interactions with DNA: mode and specificity of binding. *Biochemistry* **1993**, *32* (10), 2573−2584.

(45) Roy, S.; Hagen, K. D.; Maheswari, P. U.; Lutz, M.; Spek, A. L.; Reedijk, J.; van Wesel, P. Phenanthroline derivatives with improved selectivity as DNA-targeting anticancer or antimicrobial drugs. *ChemMedChem* **2008**, *3*, 1427−1434.

(46) Sigman, D. S.; Graham, D. R.; D'Aurora, V.; Stern, A. M. Oxygen-dependent cleavage of DNA by the 1,10-phenanthroline cuprous complex. Inhibition of *Escherichia coli* DNA polymerase I. *J. Biol. Chem.* **1979**, *254*, 12269−12272.

(47) *Bruker APEX2 version 2.1*; Bruker AXS Inc.: Madison, WI, 2008.

(48) Sheldrick, G. M. *Acta Crystallogr., Sect. A: Found. Crystallogr.* **2008**, *A64*, 112−122.

(49) Mosmann, T. Rapid colorimetric assay for cellular growth and survival: application to proliferation and cytotoxicity assays. *J. Immunol. Methods* **1983**, *65*, 56−63.

(50) Goldstein, S.; Czapski, G. Superoxide Dismutase. In *Free Radicals—A Practical Approach*; Punchard, N. A. Kelly, F. J., Eds., Oxford University Press: Oxford, UK, 1996; p 252.